THE JOURNAL OF PHYSICAL CHEMISTRY B

Article

pubs.acs.org/JPCB

Theoretical Study of Solvent Effects on the Ground and Low-Lying Excited Free Energy Surfaces of a Push−Pull Substituted Azobenzene

Jose C. Corchado,*[,†] M. Luz Sánchez,[†] Ignacio Fdez. Galván,[‡] M. Elena Martín,[†] Aurora Muñoz-Losa,[†] Rute Barata-Morgado,[†] and Manuel A. Aguilar[†]

[†]Área de Química Física, Universidad de Extremadura, Avda de Elvas s/n, 06071 Badajoz, Spain

[‡]Department of Chemistry—Ångström, The Theoretical Chemistry Programme, Uppsala University, P.O. Box 518, SE-751 20 Uppsala, Sweden

Supporting Information

ABSTRACT: The ground and low-lying excited free energy surfaces of 4-amino-4′-cyano azobenzene, a molecule that has been proposed as building block for chiroptical switches, are studied in gas phase and a variety of solvents (benzene, chloroform, acetone, and water). Solvent effects on the absorption and emission spectra and on the *cis*−*trans* thermal and photo isomerizations are analyzed using two levels of calculation: TD-DFT and CASPT2/CASSCF. The solvent effects are introduced using a polarizable continuum model and a QM/MM method, which permits one to highlight the role played by specific interactions. We found that, in gas phase and in agreement with the results found for other azobenzenes, the thermal *cis*−*trans* isomerization follows a rotation-assisted inversion mechanism where the inversion angle must reach values close to 180° but where the rotation angle can take almost any value. On the contrary, in polar solvents the mechanism is controlled by the rotation of the CN═NC angle. The change in the mechanism is mainly related to a better solvation of the nitrogen atoms of the azo group in the rotational transition state. The photoisomerization follows a rotational pathway both in gas phase and in polar and nonpolar solvents. The solvent introduces only small modifications in the $n\pi^*$ free energy surface (S_1), but it has a larger effect on the $\pi\pi^*$ surface (S_2) that, in polar solvents, gets closer to S_1. In fact, the S_2 band of the absorption spectrum is red-shifted 0.27 eV for the *trans* isomer and 0.17 eV for the *cis*. In the emission spectrum the trend is similar: only S_2 is appreciably affected by the solvent, but in this case a blue shift is found.

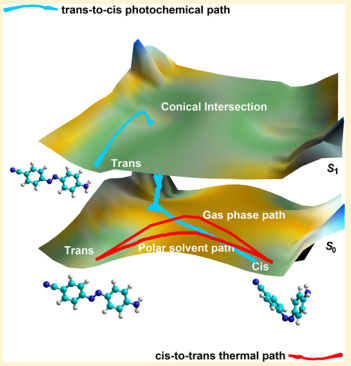

I. INTRODUCTION

Molecular structures that can undergo controlled changes or molecular switches are one of the pillars of nanotechnology. In many technological applications, optical devices or data storage for instance, it is convenient to have photoactive molecules with large dipole moment that permits, in the presence of an external electric field, to align the molecules in a particular direction. 4-Amino-4′-cyano azobenzene (ACAB) combines both characteristics and, consequently, it has been proposed as building block for chiroptical switches. This molecule and its derivatives are photoactive and they can suffer repeated *trans*−*cis*−*trans* photoisomerization cycles.[1] In addition, due to their large dipole moment, they can reorientate their axis toward a parallel alignment with the electric field of polarized light, an important property that permits to control their chiroptical behavior. Furthermore, ACAB derivatives exhibit *trans*−*cis* photoisomerization and reverse *cis*−*trans* thermal isomerization as amorphous films as well as in solution.[2]

Azobenzenes (AB) and derivatives such as ACAB have been used in molecular machines[3] due to the large geometrical differences between the *cis* and *trans* isomers. The *cis* form is significantly higher in energy than the *trans* form and the barrier to interconversion can be surmounted thermally.[4] Therefore, it can isomerize from *cis* to the more stable *trans* form both in gas or condensed phases. However, the isomerization from *trans* to *cis* cannot be achieved thermally, since the barrier to reaction is much higher.[5] Indeed, a light stimulus is required. Thus, upon photochemical excitation it is possible to achieve *trans* to *cis* isomerization, as well as *cis* to *trans*.[6] Several pathways have been proposed in order to explain photo and thermal isomerization in AB and derivatives. The first pathway is by rotation around the azo group axis, which implies changing the torsion angle CNNC labeled as ϕ in Figure 1. The second one is by inversion of any of the in-plane NNC angles, labeled as ψ_1 and ψ_2 in Figure 1. These paths can be concerted in some way, and changes in more than one angle can be significant along the reaction path. So, concerted inversion, where the two NNC angles suffer an inversion simultaneously, and inversion-assisted rotation have also been suggested as possible pathways for isomerization. Furthermore, the S_1 state can be reached by direct $n\pi^*$ (S_1) excitation, or by $\pi\pi^*$ (S_2) excitation followed by a fast decay to the S_1 state. AB photoisomerizes with a larger quantum yield when excited to S_1 than when excited to S_2.

Received: July 10, 2014
Revised: October 6, 2014
Published: October 8, 2014

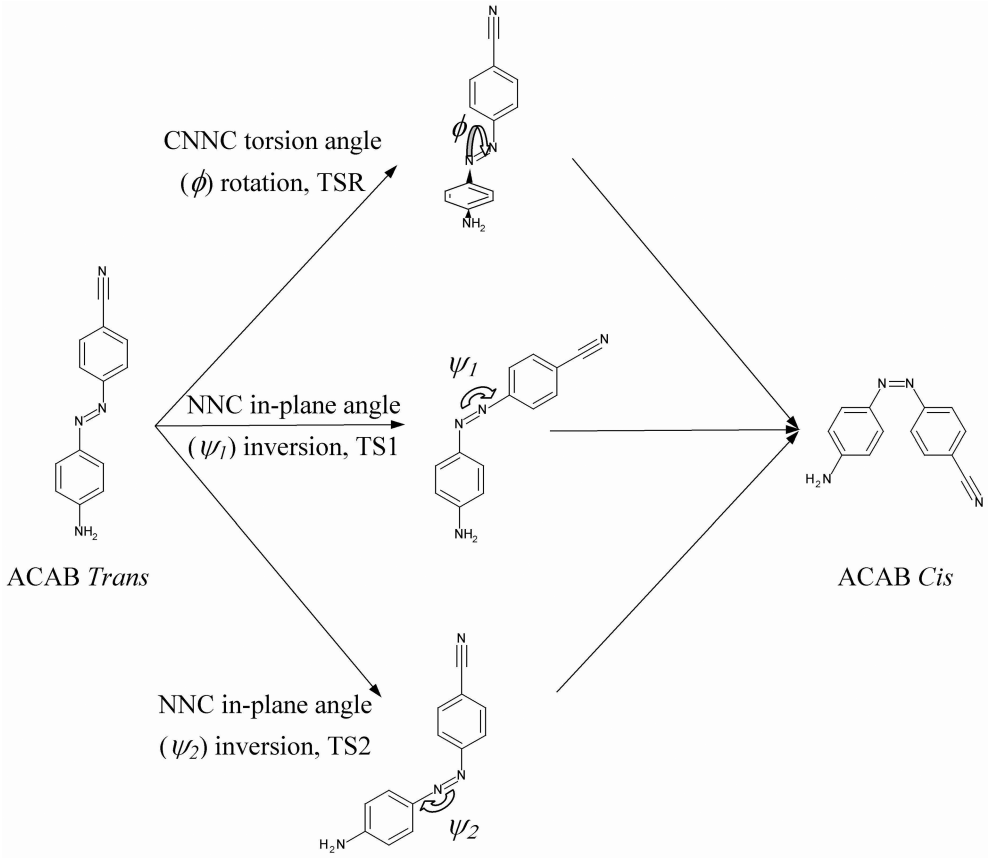

Figure 1. Mechanisms for *cis*−*trans* interconversion of 4-amino-4′-cyano-azobenzene (ACAB).

The solvent and the nature of the substituent groups can affect the isomerization mechanism both in the ground and excited state. So, for instance, in low-viscosity solvents, the S_1 state decays with a single time constant, and rotation seems to dominate the relaxation process. In more viscous solvents, the relaxation is bimodal, and the rotational pathway only contributes minimally to deactivation. Dokic et al.[7] have theoretically analyzed this question in push−pull substituted azobenzenes. They found that these compounds could undergo thermal isomerization by an inversion mechanism in gas phase and nonpolar solvents, while polar solvents seem to favor a rotational pathway. The reaction rates show a strong increase with the polarity of the solvent, besides the above-mentioned change in the pathway from inversion to rotation. Thus, rates increase by about 2 orders of magnitude when moving from heptane (ε = 1.92) to DMSO (ε = 46.7). Crecca and Roitberg[8] have theoretically studied the substituent effects on the isomerization pathway. They found that electron-donating substituents raise the ground state inversion barrier height, on the contrary, electron-withdrawing groups lower this barrier.

The conversion from the more stable *trans* form to the *cis* form can only take place by photoisomerization. This mechanism, as mentioned above, can also isomerize from *cis* to *trans* in azobenzene, but it seems not to be available on some other species, such as the bulky 3,3′,5,5′-tetra-*tert*-butyl-azobenzene on the Au(111) surface.[9] Cusati et al.[10] have recently studied the dynamics of *trans* to *cis* photoisomerization in gas phase and solution for the unsubstituted azobenzene and its competition with excited state decay. They found that, in gas phase, after excitation to the S_1 state, the ϕ torsion angle evolves from 0° (*cis*) or 180° (*trans*) to 90°, where the S_1 and S_0 surfaces meet. In this study they also show that solvent viscosity and its influence on the vibrational energy redistribution are important to understand the solvent effects on the *trans* to *cis* photoisomerization.

Despite the enormous theoretical effort devoted to the study of the thermal and photochemical isomerization in substituted and unsubstituted azobenzenes in gas and condensed phase,[8,11−34] theoretical studies on the 4-amino-4′-cyanoazobenzene are rather scarce. To the best of our knowledge, there exist only three works: the above-mentioned calculations by Dokic et al.,[5] the work by Makita et al.,[33] who made use of semiempirical calculations to explain their experimental measurements, and, more recently, that of Wang and Wang,[34] who compared AB, ACAB and ANAB (4-amino-4′-nitro-azobenzene). These authors conclude that, in gas phase, the influence of the push−pull substitution on the properties of the S_1 PES is small.

In this paper we study the ground and excited states of ACAB in gas phase and in several solvents. We discuss solvent effects both on the electronic absorption and emission spectra. We also try to shed some light on the thermal and photochemical isomerization pathways followed in different media. With this goal in mind, we have determined the potential energy surfaces of ACAB in gas phase and solvents of very different polarity, ranging from benzene (ε = 2.27) to water (ε = 78.35) using two calculation levels both for the description of the wave function (DFT and CASPT2) and the solvent effects (a polarizable continuum model, PCM, and a QM/MM method, namely ASEP/MD). The less computational-demanding level (DFT and PCM) has been used to describe in an approximate way the global free energy surface of

dx.doi.org/10.1021/jp506876v | J. Phys. Chem. B 2014, 118, 12518−12530

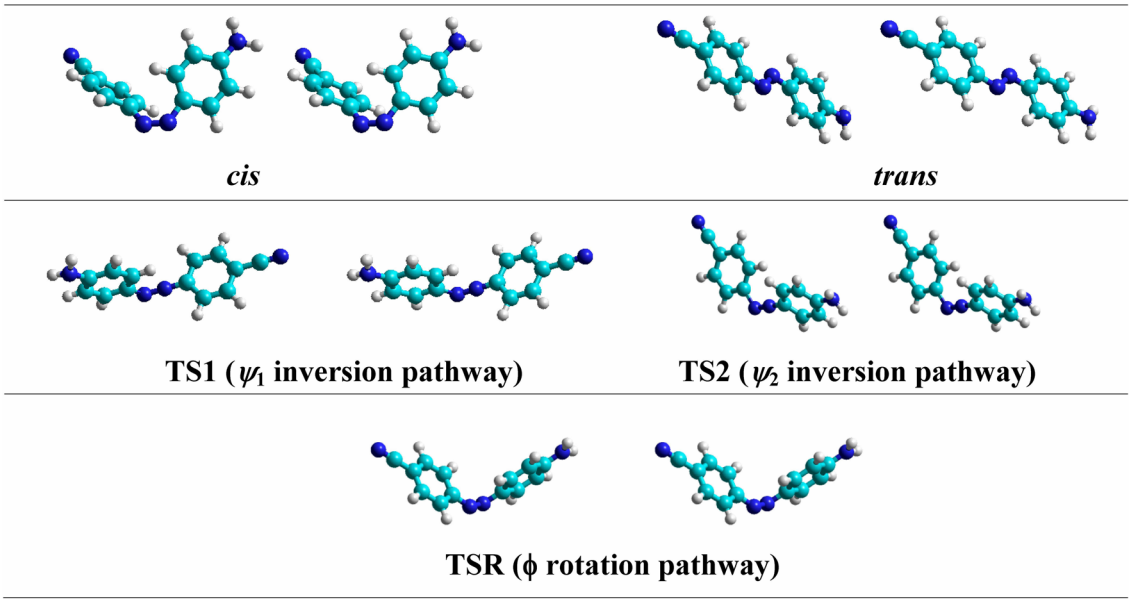

Figure 2. Stereo views of the stationary points on the ground-state surfaces.

the ground and excited states. The most accurate level (CASPT2 and ASEP/MD) has been used to characterize the critical points on the free-energy surfaces; furthermore, its comparison with DFT-PCM results allows us to check the soundness of these calculations.

II. METHODS AND COMPUTATIONAL DETAILS

In this paper, we report electronic structure calculations performed using density-functional theory (DFT) for the ground state and time-dependent density-functional theory (TD-DFT) for the excited states, employing in both cases the B3LYP hybrid funcional[35−38] and the 6-31G* basis set,[39−41] which has been shown to perform well for this system.[42]

The contour plots of the PESs were obtained by computing a grid of 190 points with the ψ_1 angle varying from 90 to 180 deg and the ϕ angle changing from 0 to 180 deg, in steps of 10°. The remaining parameters were optimized for each point. The values of the energy for ψ_1 angles in the range 180 to 270 were obtained by symmetry. Therefore, a total of 361 energies were used for each plot. The excited state PESs were obtained from vertical excitation from the ground state and, therefore, geometries were fixed to their optimized values in the ground state, and nonequilibrium solvation was added. In any case, solvent and geometry relaxation was included in selected calculations, as well as scans of the ψ_2 angle with the aim to determine the second inversion pathway and to rule out a concerted-inversion mechanism.[43]

In the most important points on the free energy surfaces (minima, conical intersections, transition states, etc.) the solute electronic transitions were recalculated using the CASPT2-(14e,12o) method at the DFT or TD-DFT optimized geometries. (For further details, see the Supporting Information.)

Solvent effects were incorporated by means of the PCM method[44] using the standard values of the radii in defining the solute cavity. For the sake of comparison, solvent effects were also described using a mean field quantum mechanics/molecular mechanics method developed in our laboratory and named ASEP/MD.[45] This method includes a detailed, microscopic description of the solvent molecules, and hence it permits one to elucidate whether specific interactions (such as hydrogen bonding) could be relevant to the description of the solvation. ASEP/MD is a QM/MM effective Hamiltonian method that makes use of the mean field approximation, that is, it introduces into the solute molecular Hamiltonian the averaged perturbation generated by the solvent. The method combines quantum mechanics (QM) and molecular mechanics (MM) techniques, with the particularity that full QM and MM calculations are alternated and not simultaneous. During the MD simulations, the intramolecular geometry and charge distribution of all the molecules are considered as fixed. From the resulting data, the average electrostatic potential generated by the solvent on the solute is obtained. This potential is introduced as a perturbation into the solute's quantum mechanical Hamiltonian, and by solving the associated Schrödinger equation, one gets a new charge distribution for the solute, which is used in the next MD simulation. The iterative process is repeated until the electron charge distribution of the solute and the solvent structure around it are mutually equilibrated. The main characteristics of the method have been described elsewhere.[46−49] (See the Supporting Information for a brief description of ASEP/MD.) It is worth noting that the solute geometry is optimized during the quantum calculation at each ASEP/MD cycle. All the calculations were performed using Gaussian 09,[50] except CASPT2 calculations that were performed using MOLCAS 7.4.[51] The molecular dynamics simulations were performed with MOLDY.[52] The molecular dynamics simulations included 660 water molecules and one molecule of solute in a cubic box of 27 Å side in order to reproduce the experimental solvent density. All molecules had fixed intramolecular geometry. For the solute, the Lennard-Jones parameters were taken from the optimized potentials for liquid simulations, all atoms (OPLS-AA) force field,[53] and the atomic charges were obtained from the quantum calculations using the CHELPG method.[54,55] For water molecules, the TIP3P model[56] was employed. Periodic boundary conditions were applied and a spherical cutoff was used to truncate interatomic interactions at 11 Å. The electrostatic interaction was calculated with the Ewald method,[57] and the temperature was fixed at 298 K with the

dx.doi.org/10.1021/jp506876v | J. Phys. Chem. B 2014, 118, 12518−12530

Table 1. Selected Geometrical Parameters of the Stationary Points on the Gas Phase S_0 Surface (in Angstroms and Degrees)

	R(N=N)	$R(C_1-N)^a$	$R(C_2-N)^a$	ψ_1	ψ_2	ϕ
cis ACAB	1.254	1.426	1.420	125.0	125.0	11.2
trans ACAB	1.267	1.415	1.400	114.2	115.5	179.9
rotational TS	n.a.	n.a.	n.a.	n.a.	n.a.	n.a.
ψ_1 inversion TS1	1.229	1.321	1.425	179.9	118.2	86.0
ψ_2 inversion TS2	1.247	1.447	1.333	116.5	178.4	104.6

[a] C_1 is the atom of the phenyl ring attached to the CN group and bonded to the azo group, while C_2 is the atom of the phenyl ring attached to the NH_2 group and bonded to the azo group.

Table 2. Potential and Free Energies at 298 K of the Stationary Points on the S_0 Surface with Respect to the *cis* Form (in kcal·mol^{-1})

	gas phase					water	
	potential energy	free energy	benzene	chloroform	acetone	PCM	ASEP/MD
cis ACAB	0.0	0.0	0.0	0.0	0.0	0.0	0.0
trans ACAB	−15.9	−15.9	−15.0	−14.7	−14.3	−14.2	−11.6
rotational TS	n.a.	n.a.	n.a.	n.a.	18.3	18.1	17.9
ψ_1 inversion TS1	19.5	18.1	19.0	18.6	n.a.	n.a.	19.1
ψ_2 inversion TS2	28.8	27.6	29.4	29.5	n.a.	n.a.	n.a.

Nose-Hoover thermostat.[58] Each simulation was run in the NVT ensemble for 75 ps, with a time step of 0.5 fs, where the first 25 ps were used for equilibration and the last 50 ps for production. In solution, final results were obtained by averaging the last five ASEP/MD cycles, and therefore they represent a 250 ps average.

III. RESULTS

A. Ground-State Potential Energy Surface in Gas Phase. Thermal Isomerization. The first step in our study was obtaining the stationary points on the gas-phase potential energy surface for the ACAB isomerization. Thus, we optimized the geometry of the *cis* and *trans* isomers as well as the saddle points of the paths connecting them at DFT/6-31G* level. Their structures are shown in Figure 2, and the most relevant geometrical parameters are given in Table 1. Born−Oppenheimer classical potential energies and free energies of these stationary points are given in the first and second columns of Table 2, respectively. Although we tried to obtain the saddle point for the rotational pathway, we could not get a stationary point along that path, and the geometry shown is that optimized in water, for the sake of completeness. We will analyze this path in deeper detail below.

First, we can see that, in agreement with X-ray data, *trans*-ACAB is planar. As for the *cis* geometry, the dihedral angle ϕ is not zero, but 11.2°. Moreover, the planes of the two benzene rings are slightly tilted in order to minimize the repulsive interactions between them. As the *cis*-to-*trans* isomerization reaction proceeds through the inversion pathways, any one of the ψ angles increases, reaching approximately 180° at the transition state. The torsional CNNC angle ϕ also changes, reaching values not far from 90° in the transition state. Therefore, this transition state is somewhat a mixture between rotational and inversion paths; we will return on this point later. When the inversion pathway follows the linearization of the ψ_1 angle, the barrier to isomerization is much lower (about 9 kcal·mol^{-1}) than when ψ_2 is the driving reaction coordinate, in agreement with the calculations of Dokic et al.[5]

As for the remaining geometrical parameters, the ψ angles in the *cis* form are slightly larger to reduce the steric repulsions. It is noticeable that during the isomerization the distance (Table 1) between the two nitrogens in the azo group decreases as well as the C−N distance of the bond involved in the linearization, while the other C−N bond is stretched.

The *trans* form is 15.9 kcal·mol^{-1} more stable than the *cis* form on the potential energy surface. The *cis*-to-*trans* isomerization takes place, as discussed above, by inversion of the ψ_1 angle, upon surmounting a barrier of 19.5 kcal·mol^{-1} on the potential energy surface. In AB these values are 12 kcal·mol^{-1} and 22 kcal·mol^{-1}, respectively. So, this combination of electron-donor and electron-withdrawing groups increases the stability of the *trans* isomer and decreases the barrier height, making the thermal *cis* to *trans* isomerization easier but the *trans*-to-*cis* isomerization more difficult than in AB. Our results reproduce the values in ref 7, which is not surprising since we are using the same calculation level, and very close to those of ref 34 obtained with B3LYP and a slightly larger basis set, and to those from CASSCF/4-31G calculations on the same paper, although the later predict a higher barrier (23.3 kcal·mol^{-1}). Note that the later results lack dynamical correlation, and the basis set is also smaller. When thermal effects at 298 K are included, while the reaction energy change is unaffected, the free energy barrier is lowered to 18.1 kcal·mol^{-1}. This is a result of a drop in the vibrational frequencies in the transition state (TS1), whose zero-point vibrational energy is about 1.0 kcal·mol^{-1} lower than that of the *cis* form. As we will see later, this TS1 is close in geometry to a conical intersection (CI). This can lead to convergence problems specially when DFT methods are used, due to the possible multiconfigurational character of the wave function. In order to check this possibility we calculated the S_0/S_1 gap at the CASPT2 level at the TS1 geometry, being 0.99 eV. The analysis of the wave function at the minima and TS1 shows an S_0 state dominated by a singlet configuration with a weight of about 0.80, with a similar weight for the dominant configuration in the S_1 excited state and without appreciable mixture of states.

Contour maps of the electronic ground-state potential energy surface, S_0, in gas phase are shown in the first panel of Figure 3. The x axis is the dihedral angle ϕ, which defines the rotational path. The y axis is the bending angle ψ_1, which defines the preferred inversion path (shown as a dotted line), consisting on the linearization of the NNC angle of the benzene ring attached

dx.doi.org/10.1021/jp506876v | J. Phys. Chem. B 2014, 118, 12518−12530

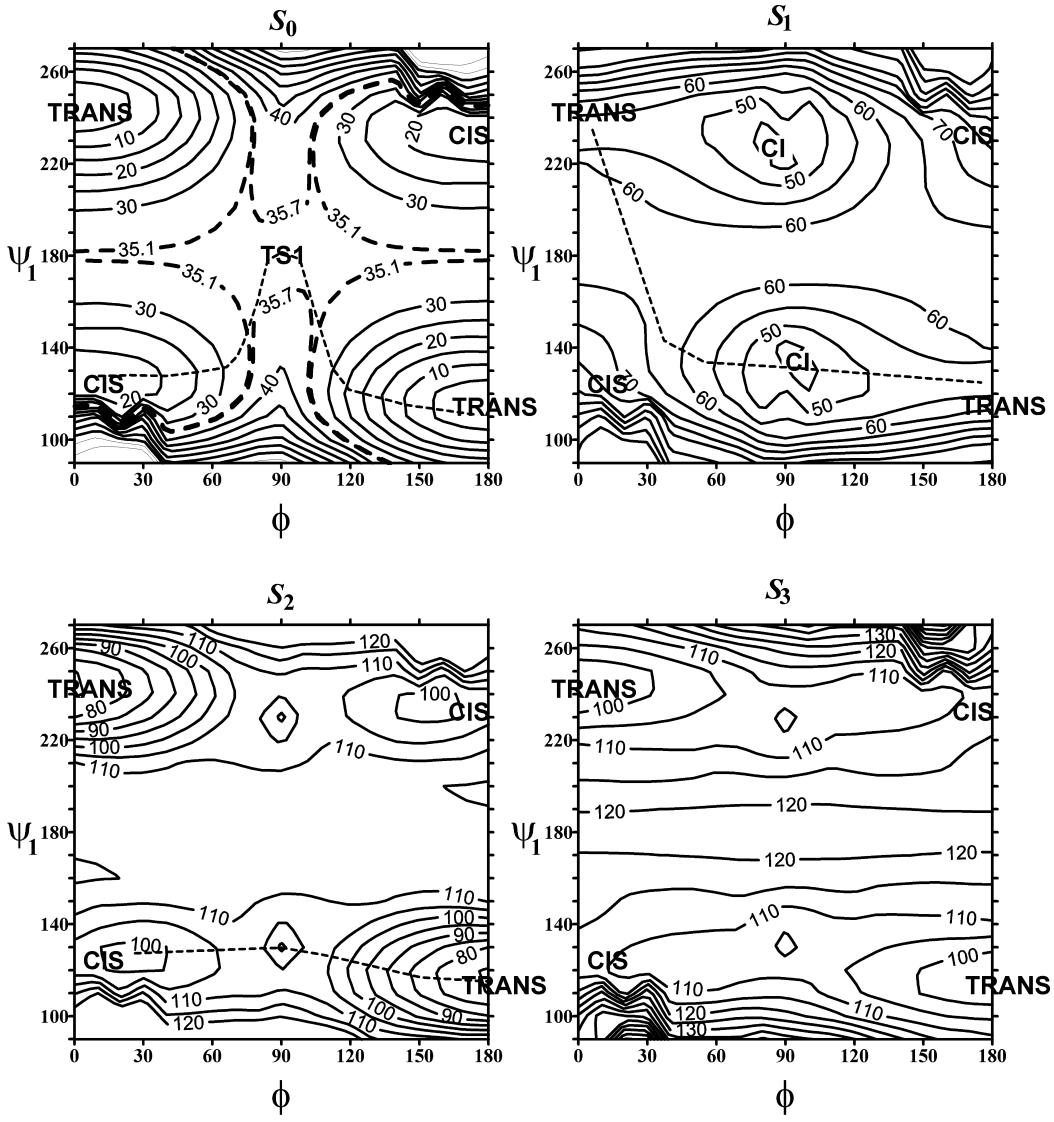

Figure 3. Contour plots of the gas-phase PESs for the four lowest electronic singlet states. The dotted lines show the minimum energy path connecting the *trans* and *cis* isomers for the S_0, S_1, and S_2 states. Note that the *cis* form is not a minimum on the S_1 PES and the path connects two *trans* forms that can interconvert. The irregular shape of the contours in the upper right corner of the plot is due to the fact that the geometry corresponding to these angles is so constrained that the geometry optimization leads to a breaking of the phenyl rings. One therefore should consider this region as unreachable because of its high energy.

to the CN group, which as we just discussed, is much lower in energy (and therefore much more thermally available) than the alternative inversion path, related to the linearization of ψ_2. Note that the saddle point energy is 35.4 kcal·mol^{-1} since the energies are shown with respect to the energy of the most stable form, the *trans* form. The dashed lines are the contours corresponding to the 35.1 and 35.7 kcal·mol^{-1} values (which is the energy of the saddle point $\pm 1/2RT$) to stress the flatness of the surface. Although from a mathematical point of view we can unquestionably locate a saddle point which predicts a rotation-inversion pathway, in the real world thermal oscillations make the paths connecting the *cis* and *trans* forms energetically available for any value of the ϕ angle. Thus, a straight line parallel to the *y* axis of the plots connecting the *cis* and *trans* forms that maintains the ϕ angle below 30° has a maximum less than 0.1 kcal·mol^{-1} higher in energy than the saddle point. Therefore, a rotation of the ϕ angle can assist the process, so that ψ_1 does not have to reach 180°, although it always has to reach a value near 180°. On the other hand, rotation around the ϕ angle without significantly linearizing the ψ_1 angle is a path too high in energy to be significant for the thermal isomerization. In sum, the thermal *cis*−*trans* isomerization follows a rotation-assisted inversion mechanism where the ψ_1 angle must reach values close to 180° but where the ϕ angle can take any value.

Finally, note that along the ψ_1 inversion reaction path in gas phase, the dipole moment increases from 7.0 D (*cis*) to 12.3 D (ψ_1 inversion transition state, or TS1) then dropping to 9.2 D in the *trans* form. Because of the large dipole moment and its changes along the reaction path, this reaction is a good candidate for studying solvent effects. For the sake of completeness, note that the TS2 transition state has a dipole moment of 8.1 D. The charge distribution, as given by the Mulliken atomic charges, are displayed in Table 3. The charges at the amino and cyano groups are very similar at the *trans* and *cis* isomers and at the TS1. Larger differences are found in the azo nitrogen atoms where the charges increase from about −0.26 au in the *cis* isomer to −0.32 au at the *trans* isomer. As

dx.doi.org/10.1021/jp506876v | J. Phys. Chem. B 2014, 118, 12518−12530

Table 3. Mulliken Atomic Charges (in a.u.) for the *cis*, *trans*, and TS1 Species in Gas Phase

	cyano group		azo group		amino group	
	C	N	N_1[a]	N_2[a]	N	H
cis ACAB	0.26	−0.44	−0.25	−0.26	−0.92	0.37
trans ACAB	0.26	−0.44	−0.33	−0.31	−0.92	0.37
ψ_1 inversion TS1	0.26	−0.45	−0.27	−0.27	−0.92	0.38

[a]N_1 is the N atom of the azo group bonded to the phenyl ring attached to the CN group, while N_2 is the N atom of the azo group bonded to the phenyl ring attached to the NH_2 group.

we will see in the next section, this fact will have effect on the relative stability of *cis* and *trans* isomers in polar solvents.

B. Solvent Effects on the Thermal Isomerization. Contour maps of the electronic ground-state potential energy surface, S_0, in chloroform and water calculated using PCM are shown in the first panels of Figures 4 and 5, respectively (similar plots for benzene and acetone are given in the Supporting Information). Energetics and selected geometrical parameters are shown in Tables 2, 4, and 5. The main criticism that can be done to dielectric continuum models as PCM is that they completely neglect the contribution of specific interactions, which can be important when the solvent is water or other associated liquids. In order to assess the soundness of PCM calculations, Table 2 also includes free-energy differences calculated with ASEP/MD and the free energy perturbation method.

First, it is interesting to note that although there are small differences between gas-phase and solution-phase, especially in the values of the ψ_1 and ψ_2 angles, the geometries of the minima on the ground-state surfaces show an almost negligible dependency on the solvent. On the other hand, as the polarity of the solvent increases, the *trans* form loses stability (with respect to the *cis* form), being the gas phase-water solvent shift about 1.7 kcal·mol^{-1}. Given that the dipole moment for the *trans* form is slightly higher than for the *cis* form, one can conclude that the solvation of ACAB is controlled by multipoles of higher order. It is worthy of note that the relative stability of the *trans* form with respect to the *cis* isomer decreases additionally by 2.6 kcal·mol^{-1} when specific

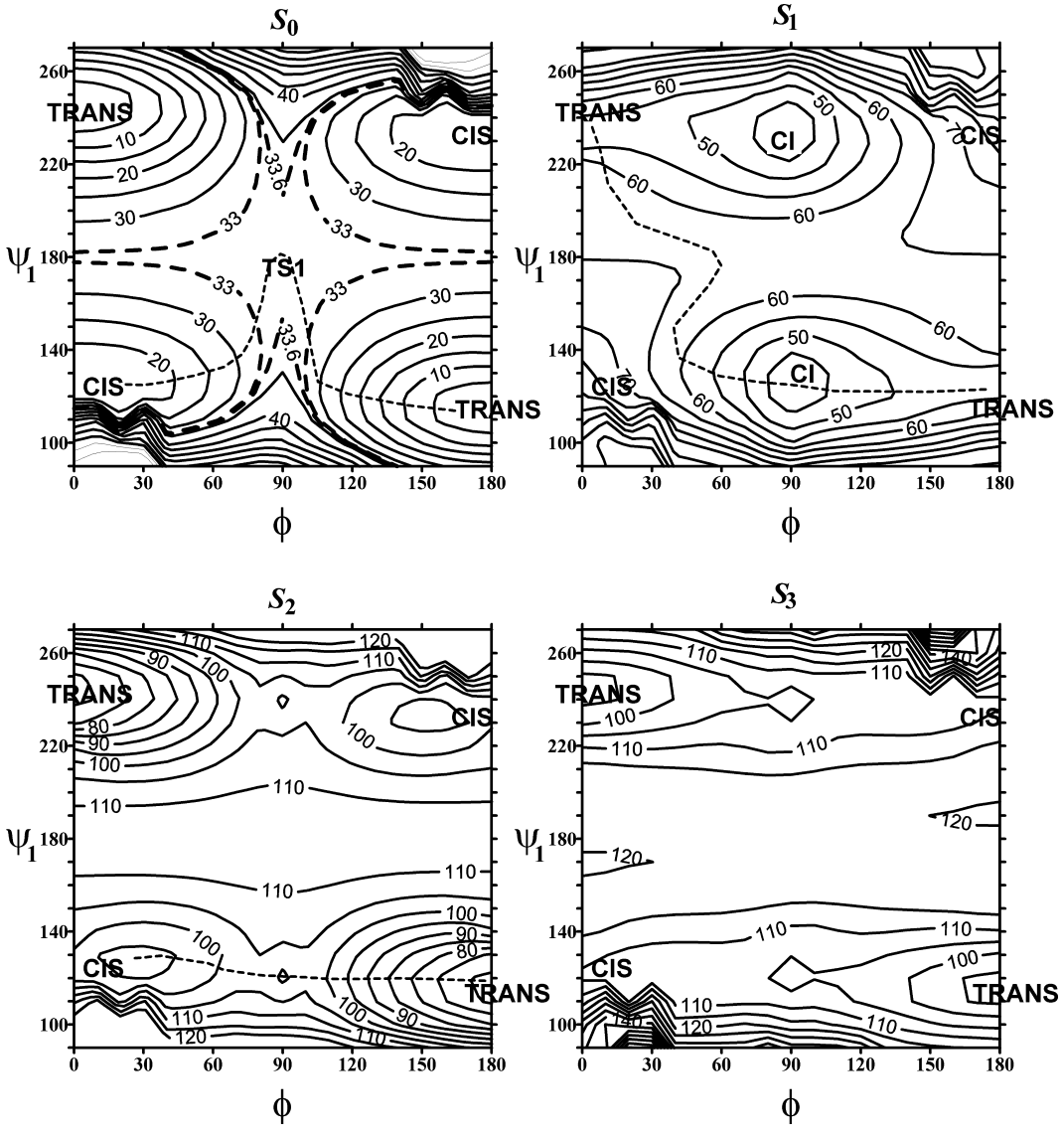

Figure 4. Contour plots of the free energy in chloroform solution for the four lowest electronic singlet states.

dx.doi.org/10.1021/jp506876v | J. Phys. Chem. B 2014, 118, 12518−12530

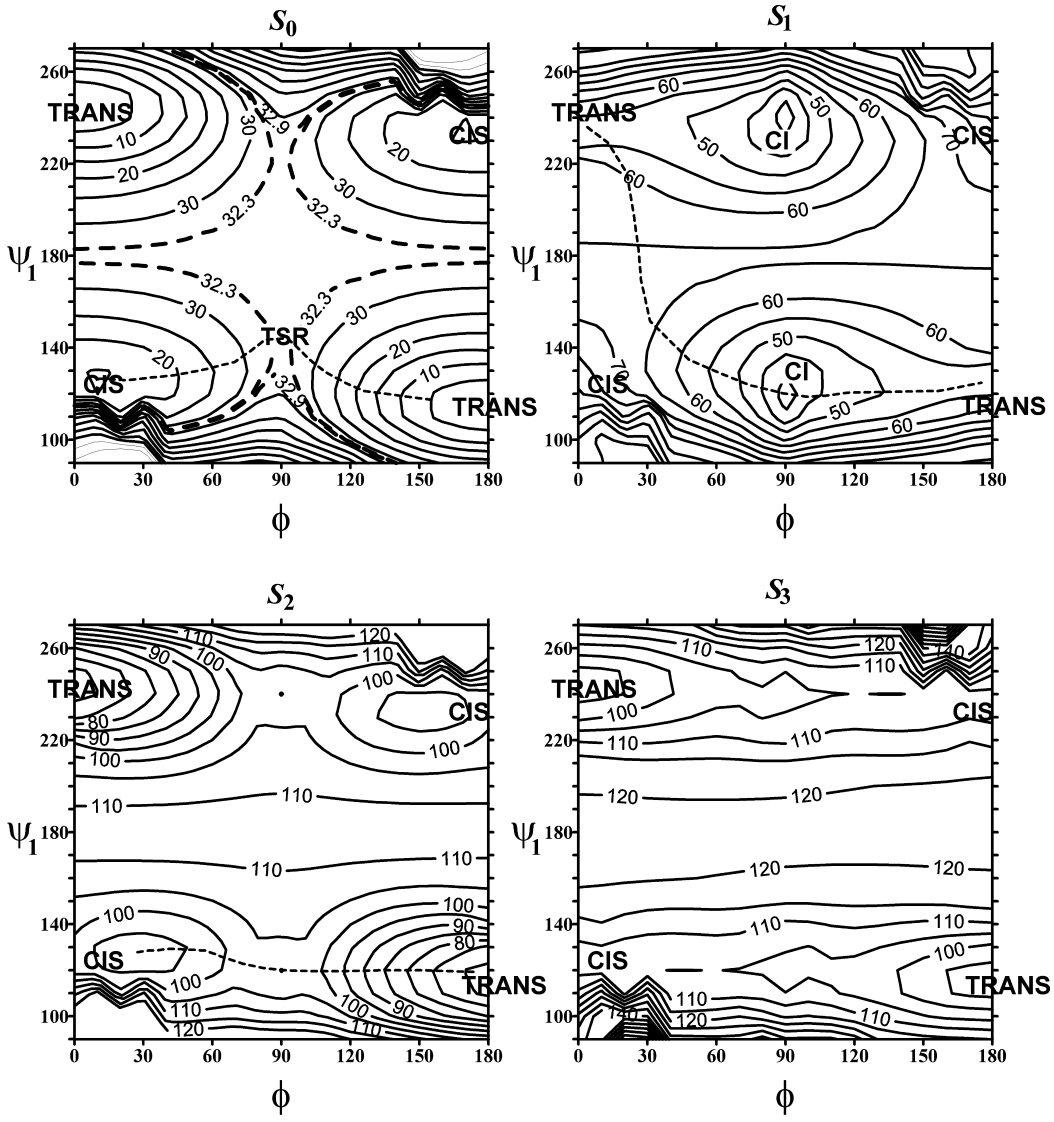

Figure 5. Contour plots of the free energy in aqueous solution for the four lowest electronic singlet states.

Table 4. Selected Geometrical Parameters of the Stationary Points on the S_0 Surface in Chloroform (in Angstroms and Degrees)

	R(N═N)	R(C$_1$–N)[a]	R(C$_2$–N)[a]	ψ_1	ψ_2	ϕ
cis ACAB	1.258	1.425	1.415	125.1	125.4	11.6
trans ACAB	1.270	1.414	1.396	114.2	115.9	179.8
rotational TS	n.a.	n.a.	n.a.	n.a.	n.a.	n.a.
ψ_1 inversion TS1	1.232	1.314	1.414	179.3	119.0	96.8
ψ_2 inversion TS2	1.255	1.445	1.333	116.5	178.1	108.0

[a]C$_1$ is the atom of the phenyl ring attached to the CN group and bonded to the azo group, while C$_2$ is the atom of the phenyl ring attached to the NH$_2$ group and bonded to the azo group.

Table 5. Selected Geometrical Parameters of the Stationary Points on the S_0 Surface in Water (in Angstroms and Degrees)

	R(N═N)	R(C$_1$–N)[a]	R(C$_2$–N)[a]	ψ_1	ψ_2	ϕ
cis ACAB	1.259	1.425	1.412	125.1	125.6	11.8
trans ACAB	1.272	1.413	1.393	114.2	116.1	180.0
rotational TS	1.274	1.324	1.367	140.4	119.6	90.7
ψ_1 inversion TS1	n.a.	n.a.	n.a.	n.a.	n.a.	n.a.
ψ_2 inversion TS2	n.a.	n.a.	n.a.	n.a.	n.a.	n.a.

[a]C$_1$ is the atom of the phenyl ring attached to the CN group and bonded to the azo group, while C$_2$ is the atom of the phenyl ring attached to the NH$_2$ group and bonded to the azo group.

dx.doi.org/10.1021/jp506876v | J. Phys. Chem. B 2014, 118, 12518−12530

interactions are included. So, the total solvent effect on the *cis*/*trans* equilibrium is 4.3 kcal·mol^{-1}.

As for the transition state, it switches from requiring a significant linearization of the ψ_1 angle (gas phase and nonpolar and slightly polar solvents) to a rotational path with smaller changes in the ψ_1 angle (strongly polar solvents). However, this is not a consequence of a dramatic change in the potential energy surface, it is caused by the smooth and subtle backdraw of the "tongue" around ϕ = 90° and ψ_1 = 140° as we move from gas phase to nonpolar solvents and to polar solvents. This "tongue" does not allow the rotational path to have a saddle point in the gas phase. Thus, the minimum energy path along the rotational pathway has to pass through an angle ψ_1 = 180°. As this "tongue" disappears, the minimum energy path passes through lower values of ψ_1 and eventually a transition state along this path appears, which is lower in energy than the inversion transition state. Thus, the value of ψ_1 at its maximum diminishes as the polarity of the solvent increases passing from 179.8° in gas phase to 140.4° in water solution. As a consequence, the thermal isomerization mechanism passes from a rotation-assisted inversion in gas phase and nonpolar solvents to an inversion-assisted rotation in polar solvents. This mechanism implies an increase of the ψ_1 of only 15° (from 125° in the *cis* isomer to 140.4° in the TSR). An important point to remark is that in water solution and due to the change in the isomerization pathway, the geometry of the TSR becomes close to a CI. In fact, the S_0/S_1 gap at the TSR geometry is only 0.63 eV at TD-DFT. When recalculated at CASPT2, the gap decreases to 0.56 eV. The analysis of the wave function along the reaction path displays similar results to those found in gas phase: the S_0 and S_1 wave functions are dominated by single configurations with a weight of 0.80 and there is no appreciable state mixing.

Figure 6 displays the radial distribution functions (rdf) between the nitrogen atoms of the cyano (panel *a*) and amino (panel *b*) groups and the oxygen atom of the water molecules, while Figure 7 displays the rdfs between the nitrogen atoms of the azo group and the oxygen atom of the water molecules (the rdf for the nitrogen atom bonded to the phenyl ring with the cyano group is shown in panel *a*, while panel *b* shows the rdf for the nitrogen atom bonded to the phenyl ring with the amino group). From these rdfs it becomes clear that the solvation of amino and cyano groups is very similar in the two transition states; however, the azo group is better solvated in TSR than in the inversion TS1. As a consequence the rotational state TSR is stabilized with respect to the inversion TS1 and the barrier to reaction in solution diminishes as the polarity of the solvent increases. In any case, the effect of the solvent on the *cis*-to-*trans* barrier height is rather small (1.4 kcal·mol^{-1} when PCM is used and 1.6 kcal·mol^{-1} when specific interactions are included), but they are significant, 5.9 kcal·mol^{-1}, for the *trans*-to-*cis* isomerization. Figure 8 compares the barrier height for the later calculated with the PCM and ASEP/MD methods. The barrier heights provided by the two solvation methods differ by about 3 kcal·mol^{-1}, the barrier height passing from 35.4 kcal·mol^{-1} in gas phase to 32.3 in water solution according to the PCM calculations or 29.5 kcal·mol^{-1} according to the ASEP/MD calculations. Therefore, the solvent effect on the barrier for the *trans*-to-*cis* isomerization predicted by the ASEP/MD method is almost twice that given by the PCM method. However, this is not enough to make the *trans*-to-*cis* thermal isomerization pathway accessible. As for the solvation of *cis* and *trans* conformers, there are important

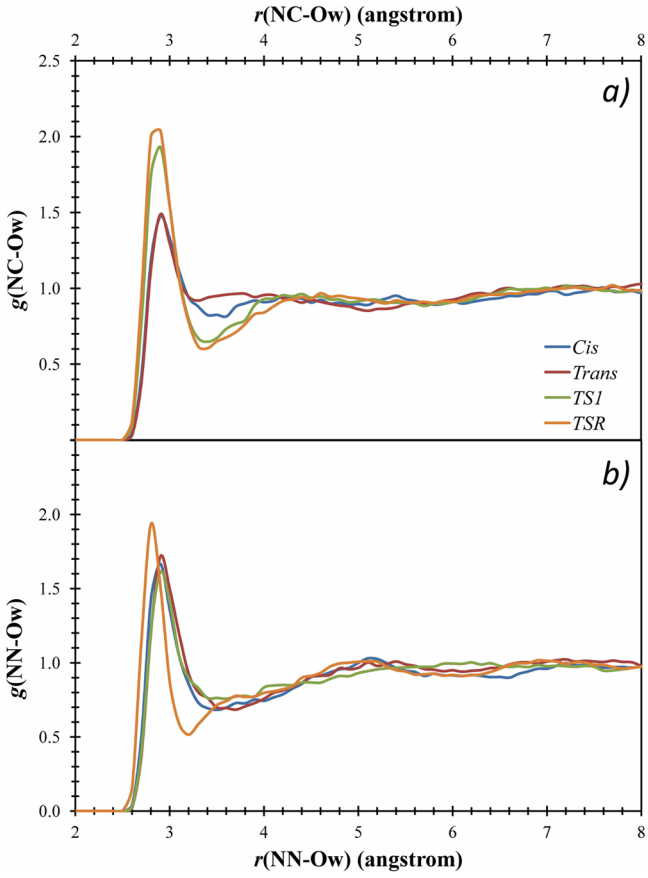

Figure 6. Radial distribution functions between the nitrogen atoms of the cyano (NAC, panel a) and amino (NAN, panel b) groups and the oxygen atom of the water molecules (Ow). TS1 indicates the inversion TS, while TSR is the rotational TS.

differences in the solvent structure around the azo nitrogen atoms (Figure 7b). These differences are due to the different accessibility of the electron lone pairs in each conformer. So, while in the *cis* isomer the electron lone pair point outward of the molecule and it can easily form hydrogen bonds with the solvent, in the *trans* isomer the lone pairs are buried inside the molecule and they cannot form hydrogen bonds due to steric hindrance.

In order to clarify the origin of the relative stability of the different structures in solution, Table 6 displays the ASEP/MD solute−solvent interaction energy and its decomposition in five group contributions: cyano, amino, azo, and the two phenyl groups. The largest solute−solvent interaction energy corresponds to the TSR, then to the *cis* isomer and, finally, to the *trans*. Both substituents, cyano and nitro groups, can form hydrogen bonds with water, but the strength of these hydrogen bonds is only slightly modified by the conformation, *cis* or *trans*, of the ACAB molecule. The nitrogen atoms of the azo group have more influence on the differential solvation of the two isomers, as these atoms form hydrogen bonds only when they are in the *cis* conformation. Note that the interaction energy of the azo nitrogen atoms with water is 19 kcal·mol^{-1} larger in the *cis* isomer than in the *trans*. In the transition state, the interaction of azo nitrogen atoms with the solvent is intermediate between the *cis* and *trans* results, but cyano and amino groups are better solvated that in the minima. The increase of the stability of the TSR with respect to the *cis* isomer is mainly due to a better solvation of the cyano group

dx.doi.org/10.1021/jp506876v | J. Phys. Chem. B 2014, 118, 12518−12530

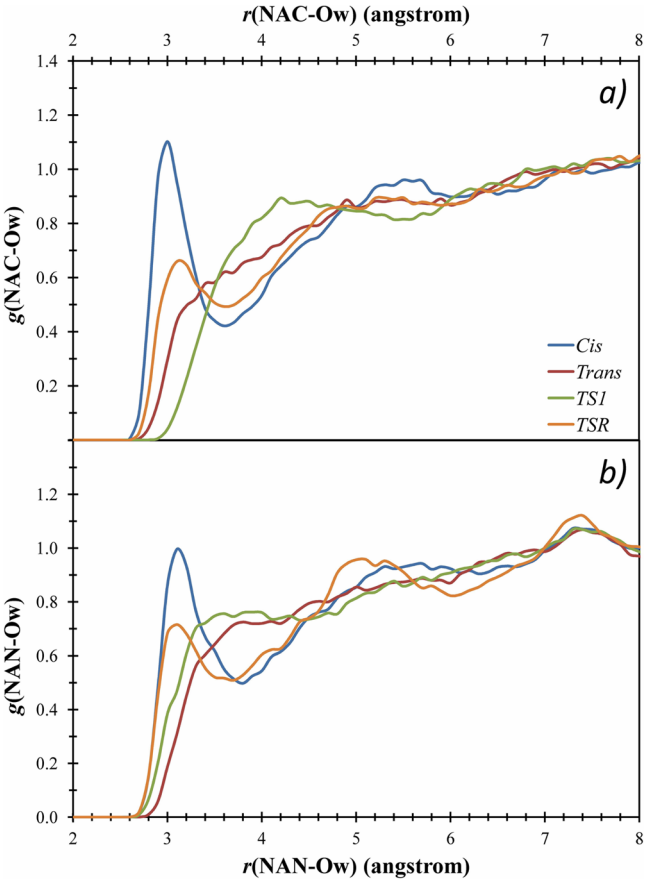

Figure 7. Radial distribution functions between the nitrogen atoms of the azo group and the oxygen atom of the water molecule (Ow). NAC (panel a) stands for the nitrogen atom bonded to the phenyl ring with the cyano group, while NAN (panel b) stands for the nitrogen atom bonded to the phenyl ring with the amino group. TS1 indicates the inversion TS, while TSR is the rotational TS.

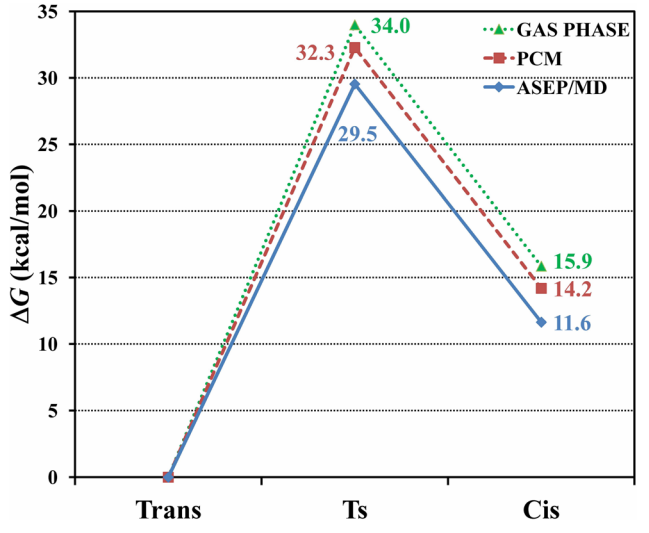

Figure 8. Schematic plot of the free energy barrier to interconversion in gas phase and aqueous solution computed using the ASEP/MD and PCM models.

and also of both phenyl rings. During the isomerization reaction, there is a transfer of water molecules from the azo group in the *cis* conformer to the neighborhood of the cyano group when the molecule is in the TSR, finally some of these hydrogen bonds are lost during the formation of the *trans* isomer. The *cis*-to-*trans* thermal isomerization implies a strong reorganization of the solvent.

Table 6. Solute−Solvent Interaction Energy (in kcal·mol^{-1}) Split up in Five Functional Groups: Cyano, Phenyl 1,[a] Azo, Phenyl 2,[a] and Amino

	cyano	phenyl 1	azo	phenyl 2	amino	total
cis ACAB	−17.7	5.4	−27.0	−2.8	−13.1	−55.1
trans ACAB	−16.9	1.6	−8.0	−2.9	−14.1	−40.2
rotational TSR	−27.5	−2.8	−10.0	−11.5	−14.9	−66.8

[a]Phenyl 1 is the phenyl ring attached to the CN group, while phenyl 2 is the ring attached to the NH_2.

Therefore, the change in the mechanism with the solvent polarity is related to (1) the larger solute−solvent interaction energy in TSR when compared with inversion TS1 and (2) the fact that the N═N distance in the rotational saddle point can reach higher values in polar solvents. As a consequence of these two factors, the area around ϕ = 90° and ψ_1 = 140° is less repulsive than in nonpolar solvents and gas-phase. In water, the N═N bond length at the TSR has a value closer to that found in the *trans* form. Thus, a longer N═N bond distance implies that the increase in the ψ_1 is not required for the interconversion of the *cis* to *trans* forms. In other words, if the N═N bond must retain its double-bond character, the ψ_1 angle has to be almost linear, and the N═N bond is shorter at the saddle point than in the minima. However, when the N═N bond elongates, the rotation become easier. Therefore, it is the solvation of the two nitrogens in the N═N bond that is responsible for the change in the mechanism. The better solvated, the more flexible it is, and the easier it is to elongate. Thus, in polar solvents, the N═N bond can rotate more easily than in nonpolar solvents, and the role of the ψ_1 angle is less important.

C. Solvent Effects on the S_1 Excited State. The potential energy profiles of the ground and low-lying excited states in gas phase and the free-energy profiles in solution are displayed in Figures 9 and 10, respectively. The main points of interest are the Franck−Condon (FC) points, which provide the absorption energy, the S_1 minima that determine the emission spectrum and the S_1 transition state and S_0/S_1 conical intersection that control the nonradiative desexcitation.

We start by analyzing the nature of the low-lying excited states. In gas phase the first excited state corresponds to an nπ^* transition. The next two states have a $\pi\pi^*$ nature. In the *cis* isomer the S_2 state displays also a certain nπ^* character, which increases in water solution, where the nπ^* character vanishes. The nature of the remaining low lying excites states is not modified by the solvent.

In gas phase and at TD-DFT level, the transitions from the *trans* ground state to the first and second excited states appear at 2.53 and 3.20 eV, respectively; while at CASPT2 they are at 2.48 and 3.56 eV. The most probable transition is to S_2, the transition probability to S_1 being 1 order of magnitude lower. For the *cis* isomer the two transitions have similar probabilities, being the transition to S_2 slightly more probable, both at the TD-DFT and CASPT2 levels of calculation. In this isomer the transitions appear at 2.51 and 3.60 eV at TD-DFT level and 2.44 and 3.82 eV at CASPT2 level. TD-DFT provides similar values for the first transition but show a trend to underestimate the transition energy to upper states in about 0.2−0.3 eV. S_2 is a

dx.doi.org/10.1021/jp506876v | J. Phys. Chem. B 2014, 118, 12518−12530

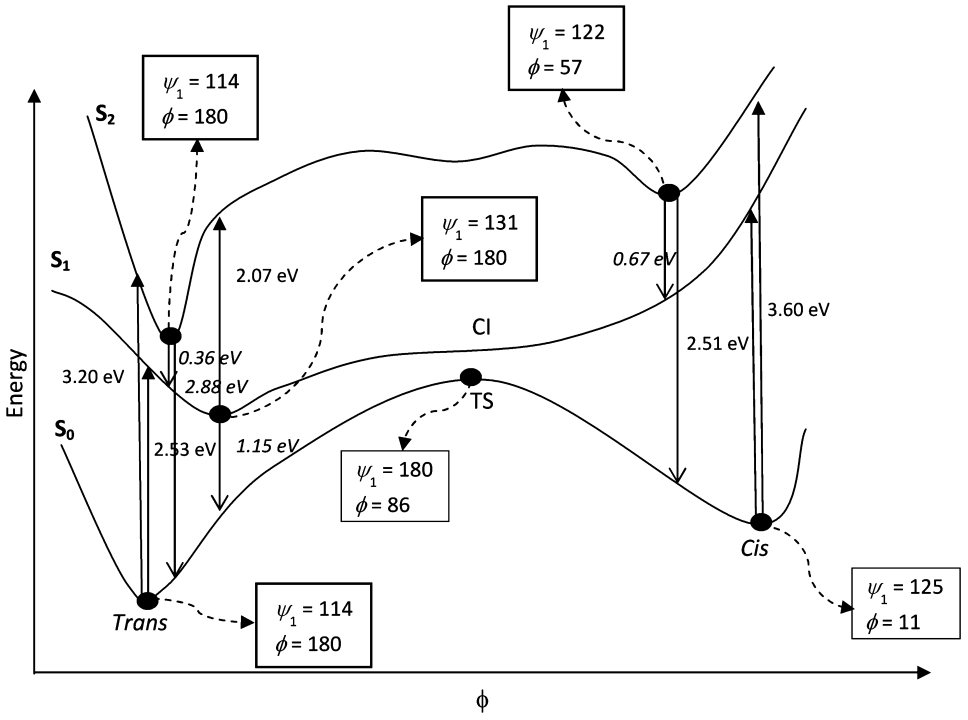

Figure 9. Schematic plot of the three lowest electronic singlet states of ACAB in gas-phase as a function of the dihedral angle ϕ. Emission values are shown in italic text while absorptions are shown in upright text. The values of the ϕ and ψ_1 angles are shown for the stationary points optimized on each electronic state.

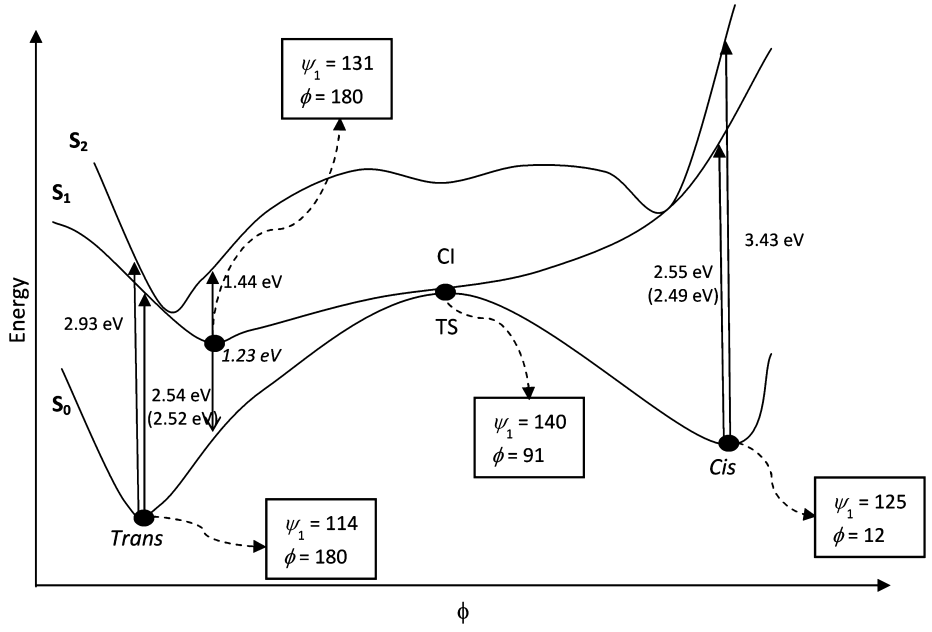

Figure 10. Schematic plot of the three lowest electronic singlet states of ACAB in aqueous solution as a function of the dihedral angle ϕ. Emission values are shown in italic text while absorptions are shown in upright text. In parentheses are shown the values obtained after solvent relaxation (for the S_1 state only). The values of the ϕ and ψ_1 angles are shown for the stationary points optimized on each electronic state assuming equilibrium solvation.

state with a multiconfigurational character, the weights of their two main configurations are 0.28 and 0.15; consequently, it is difficult to describe S_2 using TD-DFT methods. It is worth noting that the transition energy to the first excited state is almost the same in the *cis* and *trans* isomers, allowing for repeated *trans-cis-trans* photoisomerization cycles at a single wavelength. The calculated nπ^* transition energy agrees very well with the experimental values of related compounds that place this band between 2.5 and 2.8 eV. In AB, this transition appears at 2.7 eV, so there is a red shift of 0.2 eV due to the effect of the two functional groups. In gas phase the dipole moments of the S_0, S_1 and S_2 states are 9.2, 10.2, and 14.3 D for the *trans* isomer and 7.1, 6.5, and 13.5 D for the *cis*, respectively. These large dipole moments are not related with

dx.doi.org/10.1021/jp506876v | J. Phys. Chem. B 2014, 118, 12518−12530

a strong asymmetry in the charge distribution of the molecule but they are the result of small charges separated by very long distances. During the transition to S_1, changes in the charge distribution are very small. The flux of charge is larger in S_2, where electrons move from the azo nitrogen atoms and amino-phenyl group toward the cyano end of the molecule.

Due to the small differences in the charge distribution, the vertical transition energy to S_1 from the *trans* form shows a negligible change (<0.01 eV) upon solvation, but the transition energy to the S_2 state diminishes in solution. As expected, the shift in S_2 is a function of the polarity of the solvent (3.20 eV in gas phase, 2.97 eV in benzene, 2.95 eV in chloroform, and 2.93 eV in water). The gas phase/water shift is 0.27 eV that is hardly modified when specific interactions are accounted. As for the vertical excitations from the *cis* form, the findings are similar to those discussed for the *trans* form: the gap between S_0 and S_1 is only marginally affected by solvation while the gap between S_1 and S_2 diminishes in about 0.3 eV when going from gas phase to aqueous solution, as depicted in Figures 9 and 10.

It is well-known that the S_1 state of both *trans* and *cis*-AB are weakly emissive,[59] with lifetimes of 3 ps and 100 fs, respectively. A similar behavior is expected for ACAB. In fact, in gas phase, we locate a planar minimum on the S_1 excited state of *trans*-ACAB but not on the *cis* side; this could explain the differences in the S_1 lifetime of the two isomers. At TD-DFT, the emission energy from the S_1 *trans* minimum was 1.15 eV in gas phase and 1.23 eV in aqueous solution. So, the solvent now induces a small blue shift.

Once the molecules are in one of the excited states, most of them de-excite nonradiatively through a conical intersection. In gas phase, the CI (Figure 3) was located in the area near ϕ = 90° and ψ_1 = 130°. We located a transition state connecting the *trans* isomer and the CI. This TS is only 1.5 kcal·mol^{-1} above the planar minimum, which is 0.61 eV under the FC point; consequently, the TS can be easily surmounted, and the CI is accessible. Therefore, our calculations support the conclusions from other authors that there is a conical intersection at this point and, upon excitation, the system will move along the first excited state surface until it reaches this conical intersection. Then, it will fall to the ground-state surface where it will stabilize by relaxing its geometry to the *cis* or *trans* minima. In agreement with the conclusion obtained for azobenzene,[60] the rotational path would also be the preferred photoisomerization pathway for ACAB.

The shape of the S_1 PES also supports the experimental findings. Since the path from the *cis* isomer to the CI is much steeper than the path from *trans* to *cis* and the path from the CI to the *trans* form in the S_0 PES is also steeper than the path from the CI to the *cis* form, it is expected for the photochemical *cis*-to-*trans* interconversion to be faster than the *trans*-to-*cis*. Moreover, the *trans*-to-*trans* path is also possible, i.e., excitation of the *trans* form and deexcitation back to the *trans* upon rotation around the ϕ angle.

We mentioned before that when we solvate the ACAB molecule and increase the polarity of the solvent, the "tongue" in the rotational transition state area disappears and the purely rotational transition state gets stabilized. For the excited states the situation is similar, and the CI in the neighborhood of the ϕ = 90° is shifted toward lower values of the ψ_1 angle, as shown in Figure 5. Thus, for example, for aqueous ACAB a CI is located around ϕ = 90° and ψ_1 = 110°. It is important to remark that, in solution, free energy surfaces have been calculated assuming frozen solvent conditions, i.e., the solvent is in equilibrium with the ground state solute charge distribution; consequently, the CI structure found is not a true minimum-energy conical intersection (MECI). In Figure 10, on the contrary, the CI geometry has been calculated assuming the opposite limit, that is, that the solvent is always in equilibrium with the current S_1 charge distribution. The real MECI must be between these limits. In any case, and independently of the limit considered (frozen or equilibrium), we found that the solvent introduces only small changes on the topology of S_1. Furthermore, the small changes in the CI geometry do not have any effect on its energy. So, for instance, the energy difference between the groun-state of the *trans* isomer and the CI is almost the same in gas phase (0.61 eV) and in solution (0.58 eV). The same is valid for the position of the planar minimum. So, in agreement with the results found in AB, one cannot expect a significant effect of the solvent polarity on the mechanism of ACAB photochemical interconversion.

The largest solvent effects are on the S_2 surface that gets closer to the S_1 surface both at TD-DFT and CASPT2 levels. The S_2 and S_3 PESs show minima for the *trans* form, but on the S_3 PES the *cis* form is not stable (see Figures 2, 4, and 5). The *trans* minimum on the S_2 surface was fully optimized at the TD-DFT level in gas-phase. Its geometry is very similar to that of the ground-state minimum, although with the N═N bond length larger (1.319 in the S_2 surface vs 1.267 Å in S_0) and the C_1−N bond length shorter (1.368 vs 1.415 Å in S_2 and S_0, respectively). The ψ_1 and ψ_2 angles (114.3 and 110.6 degrees, respectively) are also smaller in the S_2 minima than in S_0. Note that the excitation to the S_2 state induces more significant changes in the *trans* geometry than solvation (see Tables 4 and 5), although the changes are in the same direction (the N═N bond is stretched, the C_1−N bond is shortened, and the ψ_1 and ψ_2 angles are smaller).

In AB the S_2 state can decay directly to S_0, which is a violation of Kasha's rule. If we assume the same behavior in ACAB, then an emission band must appear at 2.88 eV. From the minimum, it may also decay to the S_1 state, through an internal conversion. The gap between the S_2 minimum and S_1 decreases as the solvent polarity increases, passing form 0.36 eV in gas phase to 0.14 eV in benzene and almost 0.0 eV in water. During this photophysical process, the ϕ dihedral angle remains close to 180°, i.e., the solute is still planar. After falling to the S_1 state, the solute relaxes to the minimum on this state by rotating around the ϕ dihedral angle. When this angle is around 90°, an S_0/S_1 CI region is found, so it would relax by falling to the ground state near the transition state for the thermal interconversion. From there, it can either fall back to the *trans* form or to the *cis* form. Given that polar solvents bring S_2 closer to S_1, the kinetic energy available for the system on S_1 will be lower in polar solvents that in gas phase and nonpolar solvents, and this can affect the kinetics of the photoisomerization. It is expected that the quantum yield of the two paths, direct excitation to S_1 or excitation to S_2 followed by a fast decay to S_1, become similar in polar solvent.

Another possibility is that the system could thermally transform from *trans* to *cis* while in the S_2 state. It is interesting to note that the most probable mechanism for this excited-state interconversion would be by rotation around the ϕ angle, with a minimum in the midway, in a region near the S_0/S_1 CI and the transition state of the S_0 surface. The barrier height for the *trans*-to-*cis* interconversion would be 32.3 kcal·mol^{-1}, about 3 kcal·mol^{-1} lower than in the ground state. Moreover, the internal energy gained by relaxing from the FC geometry would

also help to this mechanism. However, the barrier height would still be too high to take this mechanism into consideration, in agreement with experiments.[61]

IV. CONCLUSIONS

In the present work we have studied the thermal and photochemical interconversion of 4-amino-4′-cyano-azobenzene in gas phase and solution. The ground-state potential energy surface is quite flat in the transition state zone, which means that the differentiation between inversion and rotational pathways for the isomerization is rather artificial, since from a dynamical point of view the two paths are thermally available. Thus, the mechanism can be defined as a rotation around the azo bond assisted by a linearization of the angle of the ring attached to the electron-withdrawing substituent. The extent of the assistance depends on the polarity of the solvent, being less important as the polarity increases. Thus, the transition state in water shows a change of only 20° in the ψ_1 angle with respect to the 120° equilibrium value, while in gas phase it becomes linear at the transition state.

TD-DFT provides a good description for the ground and S_1 states but fails to describe S_2 due to the multiconfigurational character of this state. The larger solvent effects are on S_2 that becomes close to the S_1 surface. Finally, specific interactions, although they might be significant, especially in the *cis*-to-*trans* relative stability, do not change the proposed mechanism of isomerization and, therefore, a good description of the process can be achieved using PCM.

Regarding the photochemistry of the system, although the excited-state surfaces become more stable as the solvent polarity increases, it does not seem that solvent has a strong effect either. Unfortunately, with the methods employed in the present paper, we cannot establish the impact of the solvent viscosity on the dynamics of the system, which seems to be a factor required for its proper description.

■ ASSOCIATED CONTENT

Supporting Information

A detailed description of the ASEP-MD method, additional computational details and references, as well as tables of geometrical parameters in benzene and acetone solutions, and free energy contour plots of ACAB in benzene and acetone solutions are given as Supporting Information. This material is available free of charge via the Internet at http://pubs.acs.org.

■ AUTHOR INFORMATION

Corresponding Author

*E-mail: corchado@unex.es. Phone: +34-924289300-89041.

Notes

The authors declare no competing financial interest.

■ ACKNOWLEDGMENTS

This work was supported by the GR10048 Project from the Consejería de Economía, Comercio e Innovación of the Gobierno de Extremadura. A.M.L. acknowledges financial support from the Juan de la Cierva subprogramme of the Ministerio de Economía y Competitividad of Spain. The authors also thank the Fundación Computación y Tecnologías Avanzadas de Extremadura (COMPUTAEX) for additional computational resources.

■ REFERENCES

(1) Schofield, W. C. E.; Badyal, J. P. S. Rewritable and switching chiroptical supramolecular nanolayers. *J. Mater. Chem.* **2012**, *22*, 2180−2187.
(2) Nakano, H.; Takahashi, T.; Tanino, T.; Shirota, Y. Synthesis and photoinduced surface relief grating formation of novel photoresponsive amorphous molecular materials, 4-[bis(9,9-dimethylfluoren-2-yl)amino]-4′-cyanoazobenzene and 4-[bis(9,9-dimethylfluoren-2-yl)-amino]-4′-nitroazobenzene. *Dyes Pigments* **2010**, *84*, 102−107.
(3) Balzani, V.; Credi, A.; Venturi, M. *Molecular Devices and Machines—A Journey into the Nano World*; Wiley-VCH: Weinheim, Germany, 2003.
(4) Schulze, F. W.; Petrick, H. J.; Cammenga, H. K.; Klinge, H. Thermodynamic properties of the structural analogs benzo[c]-cinnoline, trans-azobenzene, and cis-azobenzene. *Z. Phys. Chem., Neue Folge* **1977**, *107*, 1−19.
(5) Talaty, E. R.; Fargo, J. C. Thermal cis−trans-isomerization of substituted azobenzenes: A correction of the literature. *Chem. Commun.* **1967**, *2*, 65−66.
(6) Rau, H. *Photochromism: Molecular and Systems*; Durr, H., Bouas-Lauran, H., Eds.; Elsevier: Amsterdam, the Netherlands, 1990; p. 165.
(7) Dokic, J.; Gothe, M.; Wirth, J.; Peters, M. V.; Schwarz, J.; Hecht, S.; Saalfrank, P. Quantum chemical investigation of thermal cis-to-trans isomerization of azobenzene derivatives: Substituent effects, solvent effects, and comparison to experimental data. *J. Phys. Chem. A* **2009**, *113*, 6763−6773.
(8) Crecca, C. R.; Roitberg, A. E. Theoretical study of the isomerization mechanism of azobenzene and disubstituted azobenzene derivatives. *J. Phys. Chem. A* **2006**, *110*, 8188−8203.
(9) Hagen, S.; Leyssner, F.; Nandi, D.; Wolf, M.; Tegeder, P. Reversible switching of tetra-*tert*-butyl-azobenzene on a Au(1 1 1) surface induced by light and thermal activation. *Chem. Phys. Lett.* **2007**, *444*, 85−90.
(10) Cusati, T.; Granucci, G.; Persico, M. Photodynamics and time-resolved fluorescence of azobenzene in solution: A mixed quantum-classical simulation. *J. Am. Chem. Soc.* **2011**, *133*, 5109−5123.
(11) Cusati, T.; Granucci, G.; Martínez-Núñez, E.; Martini, F.; Persico, M.; Vázquez, S. Semiempirical Hamiltonian for simulation of azobenzene photochemistry. *J. Phys. Chem. A* **2012**, *116*, 98−110.
(12) Monti, S.; Orlandi, G.; Palmieri, P. Features of the photochemically active state surfaces of azobenzene. *Chem. Phys.* **1982**, *71*, 87−99.
(13) Hofmann, H.-J.; Cimiraglia, R.; Tomasi, J. A conformational basis for the description of the thermal E/Z isomerization of aromatic azo and azomethine compounds. *J. Mol. Structure (Theochem)* **1987**, *152*, 19−33.
(14) Cattaneo, P.; Persico, M. An *ab initio* study of the photochemistry of azobenzene. *Phys. Chem. Chem. Phys.* **1999**, *1*, 4739−4743.
(15) Fujino, T.; Tahara, T. Picosecond time-resolved Raman study of trans-azobenzene. *J. Phys. Chem. A* **2000**, *104*, 4203−4210.
(16) Matczyszyn, K.; Bartkowiak, W.; Leszczynski, J. Influence of the environment on kinetics and electronic structure of asymmetric azobenzene derivatives—Experiment and quantum-chemical calculations. *J. Mol. Struct.* **2001**, *565*, 53−57.
(17) Fujino, T.; Arzhantsev, S. Yu.; Tahara, T. Femtosecond time-resolved fluorescence study of photoisomerization of trans-azobenzene. *J. Phys. Chem. A* **2001**, *105*, 8123−8129.
(18) Ishikawa, T.; Noro, T.; Shoda, T. Theoretical study on the photoisomerization of azobenzene. *J. Chem. Phys.* **2001**, *115*, 7503−7512.
(19) Gagliardi, L.; Orlandi, G.; Bernardi, F.; Cembran, A.; Garavelli, M. A theoretical study of the lowest electronic states of azobenzene: The role of torsion coordinate in the cis−trans photoisomerization. *Theor. Chem. Acc.* **2004**, *111*, 363−372.
(20) Cembran, A.; Bernardi, F.; Garavelli, M.; Gagliardi, L.; Orlandi, G. On the mechanism of the cis−trans isomerization in the lowest electronic states of azobenzene: S_0, S_1, and T_1. *J. Am. Chem. Soc.* **2004**, *126*, 3234−3243.

(21) Ciminelli, C.; Granucci, G.; Persico, M. The photoisomerization mechanism of azobenzene: A semiclassical simulation of nonadiabatic dynamics. *Chem.—Eur. J.* **2004**, *10*, 2327−2341.
(22) Barada, D.; Itoh, M.; Yatagai, T. Computer simulation of photoinduced mass transport on azobenzene polymer films by particle method. *J. Appl. Phys.* **2004**, *96*, 4204−4210.
(23) Tiago, M. L.; Ismail-Beigi, S.; Louie, S. G. Photoisomerization of azobenzene from first-principles constrained density-functional calculations. *J. Chem. Phys.* **2005**, *122*, 094311.
(24) Ando, R. A.; Rodríguez-Redondo, J. L.; Sastre-Santos, A.; Fernández-Lázaro, F.; Azzellini, G. C.; Borin, A. C.; Santos, P. S. Resonance Raman spectroscopy and quantum-chemical calculations of push-pull molecules: 4-hydroxy-4′-nitroazobenzene and its anion. *J. Phys. Chem. A* **2007**, *111*, 13452−13456.
(25) de Boni, L.; Toro, C.; Masunov, A. E.; Hernández, F. E. Untangling the excited states of DR1 in solution: An experimental and theoretical study. *J. Phys. Chem. A* **2008**, *112*, 3886−3890.
(26) Sauer, P.; Allen, R. E. Influence of laser pulse parameters on dynamical processes during azobenzene photoisomerization. *J. Phys. Chem. A* **2008**, *112*, 11142−11152.
(27) Yuan, S.; Dou, Y.; Wu, W.; Hu, Y.; Zhao, J. Why does trans-azobenzene have a smaller isomerization yield for $\pi\pi^*$ excitation than for $n\pi^*$ excitation? *J. Phys. Chem. A* **2008**, *112*, 13326−13334.
(28) Conti, I.; Garavelli, M.; Orlandi, G. The different photoisomerization efficiency of azobenzene in the lowest $n\pi^*$ and $\pi\pi^*$ singlets: The role of a phantom state. *J. Am. Chem. Soc.* **2008**, *130*, 5216−5230.
(29) Ootani, Y.; Satoh, K.; Nakayama, A.; Noro, T.; Taketsugu, T. Ab initio molecular dynamics simulation of photoisomerization in azobenzene in the n π state. *J. Chem. Phys.* **2009**, *131*, 194306.
(30) Lee, Y. J.; Yang, S. I.; Kang, D. S.; Joo, S.-W. Solvent dependent photo-isomerization of 4-dimethylaminoazobenzene carboxylic acid. *Chem. Phys.* **2009**, *361*, 176−179.
(31) Wang, L.; Wu, W.; Yi, C.; Wang, X. Isomerization and electronic relaxation of azobenzene after being excited to higher electronic states. *J. Mol. Graphics Modell.* **2009**, *27*, 792−796.
(32) Tiberio, G.; Muccioli, L.; Berardi, R.; Zannoni, C. How does the trans−cis photoisomerization of azobenzene take place in organic solvents? *ChemPhysChem* **2010**, *11*, 1018−1028.
(33) Makita, S.; Saito, A.; Hayashi, M.; Yamada, S.; Yoda, K.; Otsuki, J.; Takido, T.; Seno, M. Electronic spectra of push−pull 4-phenylaminoazobenzene derivatives. *Bull. Chem. Soc. Jpn.* **2000**, *73*, 1525−1533.
(34) Wang, L.; Wang, X. Ab initio study of photoisomerization mechanisms of push−pull *p,p′*-disubstituted azobenzene derivatives on S_1 excited state. *J. Mol. Struct. (THEOCHEM)* **2007**, *847*, 1−9.
(35) Becke, A. D. Density-functional thermochemistry. III. The role of exact exchange. *J. Chem. Phys.* **1993**, *98*, 5648−5652.
(36) Lee, C.; Yang, W.; Parr, R. G. Development of the Colle−Salvetti correlation-energy formula into a functional of the electron density. *Phys. Rev. B* **1988**, *37*, 785−789.
(37) Vosko, S. H.; Wilk, L.; Nusair, M. Accurate spin-dependent electron liquid correlation energies for local spin density calculations: A critical analysis. *Can. J. Phys.* **1980**, *58*, 1200−1211.
(38) Stephens, P. J.; Devlin, F. J.; Chabalowski, C. F.; Frisch, M. J. Ab Initio calculation of vibrational absorption and circular dichroism spectra using density functional force fields. *J. Phys. Chem.* **1994**, *98*, 11623−11627.
(39) Ditchfield, R.; Hehre, W. J.; Pople, J. A. Self-consistent molecular-orbital methods. IX. An extended gaussian-type basis for molecular-orbital studies of organic molecules. *J. Chem. Phys.* **1971**, *54*, 724−729.
(40) Hehre, W. J.; Ditchfield, R.; Pople, J. A. Self-consistent molecular orbital methods. XII. Further extensions of gaussian-type basis sets for use in molecular orbital studies of organic molecules. *J. Chem. Phys.* **1972**, *56*, 2257−2261.
(41) Hariharan, P. C.; Pople, J. A. The influence of polarization functions on molecular orbital hydrogenation energies. *Theoret. Chim. Acta* **1973**, *28*, 213−222.
(42) Biswas, N.; Umapathy, S. Density functional calculations of structures, vibrational frequencies, and normal modes of trans- and cis-azobenzene. *J. Phys. Chem. A* **1997**, *101*, 5555−5566.
(43) Diau, E. W.-G. A new trans-to-cis photoisomerization mechanism of azobenzene on the $S_1(n,\pi^*)$ surface. *J. Phys. Chem. A* **2004**, *108*, 950−956.
(44) Tomasi, J.; Mennucci, B.; Cammi, R. Quantum mechanical continuum solvation models. *Chem. Rev.* **2005**, *105*, 2999−3093.
(45) Fdez. Galván, I.; Sánchez, M. L.; Martín, M. E.; Olivares del Valle, F. J.; Aguilar, M. A. ASEP/MD: A program for the calculation of solvent effects combining QM/MM methods and the mean field approximation. *Comput. Phys. Commun.* **2003**, *155*, 244−259.
(46) Sánchez, M. L.; Aguilar, M. A.; Olivares del Valle, F. J. Study of solvent effects by means of averaged solvent electrostatic potentials obtained from molecular dynamics data. *J. Comput. Chem.* **1997**, *18*, 313−322.
(47) Sánchez, M. L.; Martín, M. E.; Aguilar, M. A.; Olivares del Valle, F. J. Solvent effects by means of averaged solvent electrostatic potentials: Coupled method. *J. Comput. Chem.* **2000**, *21*, 705−715.
(48) Muñoz Losa, A.; Fdez. Galván, I.; Martín, M. E.; Aguilar, M. A. Theoretical study of liquid hydrogen fluoride. Application of the averaged solvent electrostatic potential/molecular dynamics method. *J. Phys. Chem. B* **2003**, *107*, 5043−5047.
(49) Sánchez, M. L.; Martín, M. E.; Fdez. Galván, I.; Olivares del Valle, F. J.; Aguilar, M. A. Theoretical calculation of the Stark component of the solute-solvent interaction energy. Validity of the mean field approximation in the study of liquids and solutions. *J. Phys. Chem. B* **2002**, *106*, 4813−4817.
(50) Frisch, M. J.; Trucks, G. W.; Schlegel, H. B.; Scuseria, G. E.; Robb, M. A.; Cheeseman, J. R.; Scalmani, G.; Barone, V.; Mennucci, B.; Petersson, G. A.; et al.. *Gaussian 09*, revision A.1; Gaussian Inc.: Wallingford, CT, 2009.
(51) Aquilante, F.; de Vico, L.; Ferré, N.; Ghigo, G.; Malmqvist, P.-Å.; Neogrády, P.; Pedersen, T. B.; Pitoňák, M.; Reiher, M.; Roos, B. O.; et al. Software news and update MOLCAS 7: The next generation. *J. Comput. Chem.* **2010**, *31*, 224−247.
(52) Refson, K. Moldy: A portable molecular dynamics simulation program for serial and parallel computers. *Comput. Phys. Commun.* **2000**, *126*, 310−329.
(53) Jorgensen, W. L.; Maxwell, D. S.; Tirado-Rives, J. Development and testing of the OPLS all-atom force field on conformational energetics and properties of organic liquids. *J. Am. Chem. Soc.* **1996**, *118*, 11225−11236.
(54) Chirlian, L. E.; Francl, M. M. Atomic charges derived from electrostatic potentials: A detailed study. *J. Comput. Chem.* **1987**, *8*, 894−905.
(55) Breneman, M.; Wiberg, K. B. Determining atom-centered monopoles from molecular electrostatic potentials. The need for high sampling density in formamide conformational analysis. *J. Comput. Chem.* **1990**, *11*, 361−373.
(56) Jorgensen, W. L.; Chandrasekhar, J.; Madura, J. D.; Impey, R. W.; Klein, M. L. Comparison of simple potential functions for simulating liquid water. *J. Chem. Phys.* **1983**, *79*, 926−935.
(57) Allen, M. P.; Tildesley. D. J. *Computer Simulation of Liquids*; Oxford University Press: London, 1987.
(58) Hoover, W. G. Canonical dynamics: Equilibrium phase-space distributions. *Phys. Rev. A* **1985**, *31*, 1695−1697.
(59) Stuart, C. M.; Frontiera, R. R.; Mathies, R. A. Excited-state structure and dynamics of cis- and trans-Azobenzene from resonance Raman intensity analysis. *J. Phys. Chem. A* **2007**, *111*, 12072−12080.
(60) Altoè, P.; Bernardi, F.; Conti, I.; Garavelli, M.; Negri, F.; Orlandi, G. Light driven molecular switches: Exploring and tuning their photophysical and photochemical properties. *Theor. Chem. Acc.* **2007**, *117*, 1041−1059.
(61) Bandara, H. M. D.; Burdette, S. C. Photoisomerization in different classes of azobenzene. *Chem. Soc. Rev.* **2012**, *41*, 1809−1825.